

Real-Time Print Quality Diagnostics

Zuguang Xiao^a, Minh Nguyen^a, Eric Maggard^b, Mark Shaw^b, Jan Allebach^a, Amy Reibman^a

^aSchool of Electrical and Computer Engineering, Purdue University, West Lafayette, IN 47906, U.S.A.

^bHP Inc., Boise, ID 83714, U.S.A.

Abstract

The traditional diagnostics of print quality requires to print a professionally designed test-page and visually evaluated by an expert, which is very costly and time-consuming [14]. Instead, a system that could automatically diagnose a customer's printer without any human's interference is proposed in this paper¹. The system relies on scanning user's printed output from user's printer. Print defects such as banding, streaking, etc. will be reflected on its scanned page and can be captured by comparing to its master image. The master image is the digitally generated original from which the page is printed. Once the print quality drops below a specified acceptance criteria level, the system can notify the user of the presence of print quality issues.. The current process has only concentrated on one type of print defect: text fading. The scanned page will initially be aligned with its master image with a feature based image registration algorithm. Text regions of the two pages are then extracted and compared directly.

1.0 Introduction

A prototype system was built in which scanner was used to scan select pages. The scanned image, or images, will be used for comparison and analysis of the printed image. The scanning module and image processing are done on a workstation.

The overall system flow is shown in Figure 1. The system is listening to the printer firmware, and an event will be received by the system whenever a print job is issued. Once the event is received, the scanner is initialized to get ready to scan the print-out coming out from the printer. The scanned page along with calibrated master image retrieved from the firmware will be processed by the image processing block. It is possible that the image processing block takes much longer than the page throughput for multipage jobs, so that as the current page is being processed, a new page arrives before the system is ready. This can be solved by disabling the system from listening to the firmware until the current analysis is finished. However, this means that even though the customer's print quality is being monitored in real-time, not every print page needs to be scanned and analyzed.

The scanned page may be subject to translation, scaling, skewing. So to compare the scanned image with the scanner calibrated master image, we have to spatially align them. This is done by a global image registration algorithm. Some image registration algorithm, like Fourier based method [19][20] usually yields poor result for our application. This is due to our target, the scanned page, potentially being distorted with print defects and containing high frequency noise of halftone patters. Therefore a feature based image registration algorithm was selected

Our text fading detection bases on the work of Ju [16] et

¹Research supported by HP Inc., Boise, ID 83714

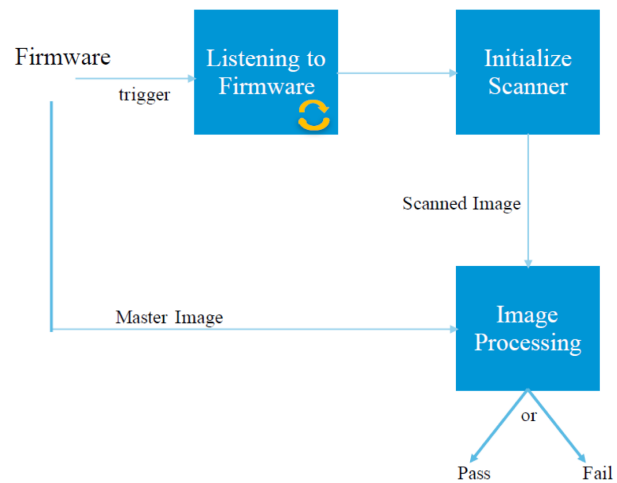


Figure 1: System Process Flow.

al. In that work, they compared a text faded page with the paper white for each text character by calculating the mean ΔE in $L^* a^* b^*$ color space. The histogram of all the characters of the whole page will appear diverged if some of the text characters are faded. If there is no fading, or all the characters are faded, then histogram will appear more concentrated. Two shortcomings exist in this method. First, if a page contains text characters with different colors, then the mean ΔE for different color text characters could vary, and the histogram will become diverged. Second, if the page has very little fading, then these faded characters will not affect the overall histogram too much since they only account for a very small population; but these fading characters are still noticeable to human eyes. To address the first problem, because of the availability of the master image, we could directly calculate the mean ΔE between the scanned image and the master image for each character. This comparison requires to convert the master image to scanner RGB first. Second problem can be dealt by dividing the page to several blocks or strips, and locally evaluate the histogram for each block or strip instead of the whole page. Therefore, when even a small number of text characters have fading, the local region histogram will diverge.

This work builds on recent image quality work focused on printer and scanner products that was conducted in our laboratory, and which addressed assessment of page non-uniformity [1]-[6], fine-pitching banding [7]-[11], ghosting [12], local defects [13],[14], fading [15],[16], scanner MTF [17], and scanner motion quality [18].

2.0 Image Registration

2.1 Methodology

Feature based image registration algorithm involves of finding feature points, for example corners, of objects in two images and calculating a best match between the features. The features can be used to establish point to point correspondence and geometric transformation can be estimated [21]. The geometric transformation is applied to the target image to spatially align with the source image.

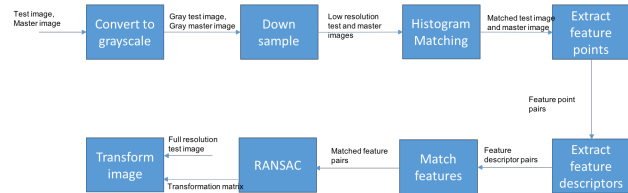


Figure 2: Image Registration Algorithm.

Figure 2 shows the overall image registration algorithm. The input scanner RGB test image and master firmware image are converted to grayscale first, then they are downsampled to a lower resolution for faster computation. Without considering the histogram matching block at this moment, feature points can be extracted from these low resolution grayscale images. There are various types of feature point; the most simple and basic feature point detector is the Harris corner [22] with sub-pixel accuracy [23]. Harris corners can be summarized as the expressions in Figure 3, where I is the input image; I_x and I_y are the partial derivatives with respect to x and y ; G is the Gaussian filter; K is the sensitivity factor; CSF is the corner strength function. $CSF(x,y)$ will be large when there is strong gradient along both x direction and y direction at point (x,y) , and it's close to zero at smooth area. Points whose corner strength are larger than a threshold are selected as feature interest points. The main drawback of Harris corners is that it fails to deal with scale changes [24], but that is not a problem here, since the test and the master image are always at the same scale.

$$I_x = I * \begin{bmatrix} -1 & 0 & 1 \end{bmatrix}; I_y = I * \begin{bmatrix} -1 & 0 & 1 \end{bmatrix};$$

$$I_x I_y = I_x \cdot I_y;$$

$$I_x^2 = I_x^2 * G; I_y^2 = I_y^2 * G; I_x I_y = I_x I_y * G;$$

$$CSF(x,y) = (I_x^2 \cdot I_y^2 - (I_x I_y)^2) - k \cdot (I_x^2 + I_y^2)^2$$

Figure 3: Harris Corners.

After acquiring the feature points, feature descriptors can be extracted at each feature point. If we assume that the test image is skewed by only a small angle with respect to the master image, we could simply extract a block of pixels centered at each feature point as the feature descriptors. Notice this feature descriptors work very poorly when the skew angle is large. The extracted feature descriptors can be matched with Squared Sum of intensity Differences (SSD), and SSD is preferred when there is small variation in intensity between images [25]. However, the test image, which maybe distorted with text fading, could have a very different intensity with respect to master image. Matching accuracy can be greatly improved if the histogram of test image

is matched with the master before the feature matching. Another difficulty to achieve accurate matching happens when the test and master image contain only text. A text character that is on the top of a test image may be matched with the same text character that appears in the middle or bottom of the master image. This can be solved by limiting the spatial distance between the feature pairs being matched.

A geometric transformation matrix, like affine can be estimated from the matched pairs with RANSAC [26], or the more robust method MLESAC [27]. The estimated transformation matrix will be applied to the full resolution test image instead of the low resolution test image. The translation parameters in the transformation matrix will need to be scaled up by the downsampling rate before being applied.

2.2 Experiment Result

Figure 4 shows a test image and the master firmware image overlapping with each other. They both have a resolution of about 3200 x 2464 at a spatial resolution of 300 dpi. It can be seen that they are misaligned both vertically and horizontally. Both the test image and the master image are converted to grayscale and then downsampled by 4 in both vertical and horizontal directions. This results in two 800 x 600 low resolution images as shown side by side in Figure 5. Feature points are extracted from both lower resolution images and are matched. The color circles are the feature points and the feature pairs connected by straight lines are matched. As can be seen from Figure 5, there are several mismatched pairs in the top half of the image. Even with some mismatched feature pairs, these outliers can be rejected by the RANSAC or MLESAC algorithm.

Figure 6 shows the transformed full resolution test image overlapped with the master image. The global alignment algorithm in general yields good results, however, on the top right corner of the page, we can still see a little misalignment, which is about 10-pixels. For more than 30 pages we have tested, we could achieve, on average, alignment within 15-pixels. To achieve a better alignment, a localized alignment was done during the text fading portion of the analysis.

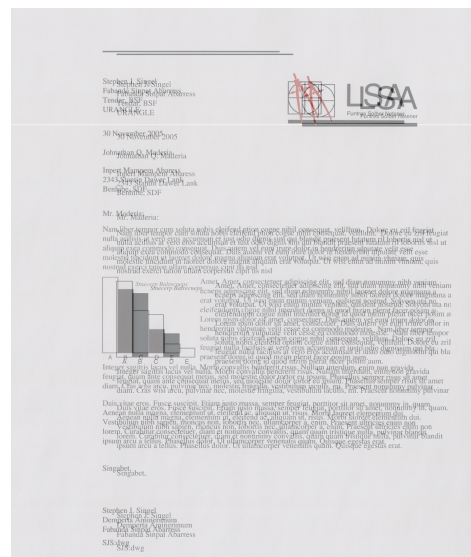


Figure 4: Before alignment.

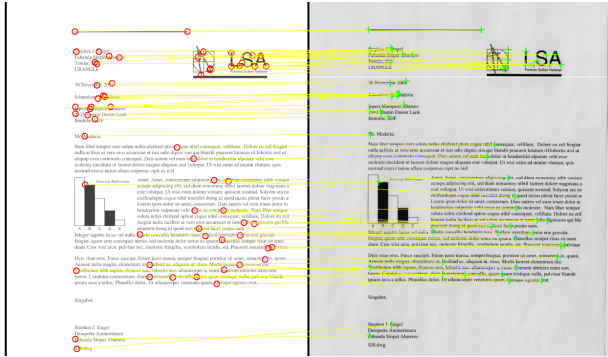


Figure 5: Matched feature pairs.

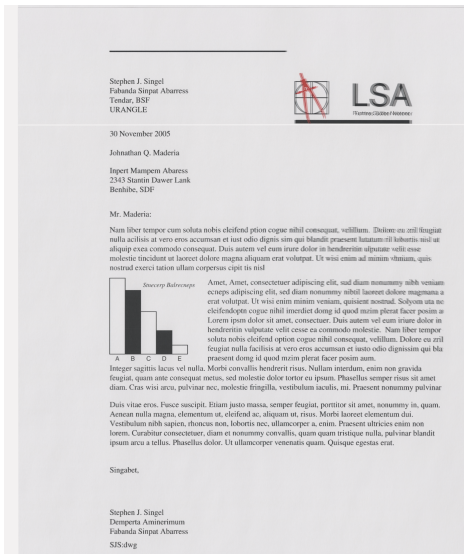


Figure 6: After alignment.

3.0 Text Fading Detection Algorithm

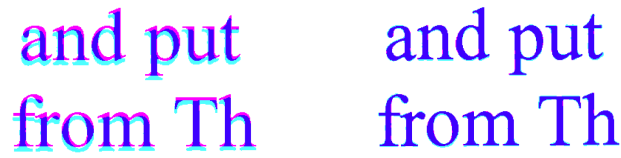
3.1 Local Alignment

Our text fading detection algorithm is based on calculating the color difference for all the text character pixels. As discussed previously, our image registration algorithm could not achieve perfect pixel to pixel alignment; and as far as we know, there is no algorithm can achieve that for such a large image. So to compare pixel in the test image with the same pixel in the corresponding location in the master image, we have to extract all the text characters and locally align them. The algorithm flow is described in Figure 7.

The adaptive thresholding will binarize a gray image, separating text characters from the background. The pixels in the text characters are connected by the connected component algorithm, and morphological operation is performed to remove noises. Only the master's text characters components are extracted, and for each extracted component, it will be used as a template to find a match in the test binary image inside a localized range. The searching range completely depends on how accurately these two images are registered during the previous step. Figure 8 shows the local alignment result; each character of the master image is now perfectly matched with the test image. At the end of this process, we will have a list of components of text characters, and each component contains a pixel list that can be used for pixel-wise color comparison.



Figure 7: Local alignment.



(a) Before local alignment.

(b) After local alignment

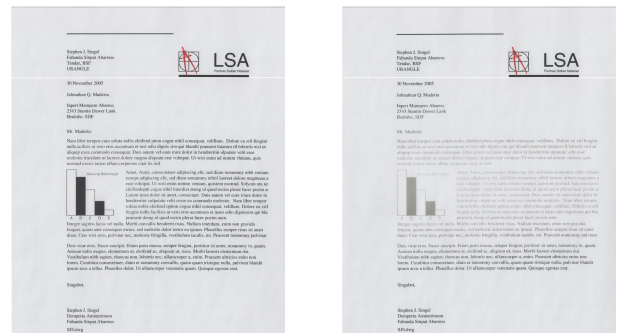
Figure 8: Cyan is the test binary image; magenta is the master binary image, and blue is overlapping.

3.2 Color Comparison

To compare the difference between two colors, the most commonly used metric is ΔE , which is the Euclidean distance between two points in $L^* a^* b^*$ color space. The pixel list extracted previously is in scanner calibrated RGB and will be needed to convert to $L^* a^* b^*$ first, and then ΔE will be calculated for each pixel in the list between the master and the test images. Notice this is more efficient than converting the whole page pixels from scanner RGB color space to $L^* a^* b^*$ color space. The mean ΔE for each pair of components/characters indicate their perceptual difference on average. When a text character is faded, no matter what color it is, the mean ΔE will become very large.

3.3 Statistical Analysis

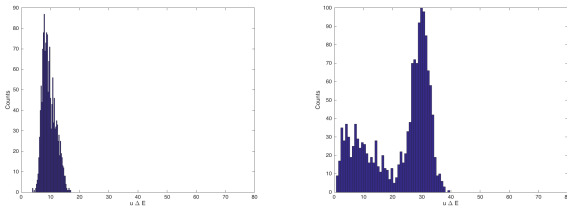
If we plot the histogram of the mean ΔE of all the characters, an unfaded page, like Figure 9(a), will exhibit a very narrow spread histogram as shown in Figure 10(a). In contrast, when fading exist, like the sample in Figure 9(b), not only its histogram, Figure 10(b), will spread out, but also the mean will shift to right (a larger value). However, the histogram will become less dispersed as well when the whole page if faded. Therefore, we could just use the mean of the mean ΔE as the measure of the fading level. Consider the situation when we only have a very narrow strip of text characters that are faded, then the mean of the mean ΔE in a large degree will be dominated by the larger population of non faded text characters. The fading can be more easily detected if we divide a page to many small regions, for example strips, and then analyze the mean of mean ΔE locally for each region.



(a) test image without fading.

(b) test image with fading

Figure 9: Test samples.



(a) Histogram of none faded page (b) Histogram of faded page
Figure 10: Histogram of test images.

3.4 Experiment Result

A series of test pages with increasing level of text fading are shown in Figure 11(a)(c)(e)(g). For visualization purpose, all the test pages are divided into four horizontal strips; in practice, we divided them into eight strips or more depending on the type of page being analyzed. The histogram plotted to the right of each test page is the distribution of the mean ΔE for each character in each strip compared with a master page, which is not shown here.

The first page, Figure 11(a) is near an unfaded page. As we can see from its histograms in Figure 11(b), they are all very narrow, and their peaks are located at their means, which are all less than 10. When fading starts to arise in the middle two strips, shown in Figure 11(c), the middle two histograms in 11(d) start to spread to the right, and their means become larger. For the strips that there are no fading, their histograms remain almost unchanged. As the fading level increases, the histogram will further shift to the right. For the last test page, Figure 11(g), where almost all the text characters in the middle two strip are faded, their histograms, Figure 11(h), are less dispersed compared with 11(f), and the new peaks are located around 35.

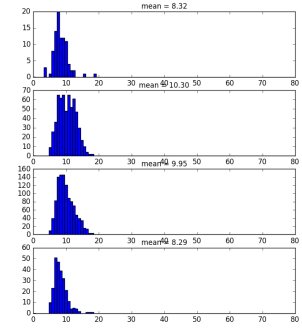
The system can scan and process a full letter sized text page in about 5 to 7 seconds. This result is from the system on the workstation.

4.0 Conclusion

In conclusion, this paper proposed a real-time print quality diagnostic system. The system requires a scanner to scan customer's printout. The scanned image is then globally aligned with its master image by using a feature based image registration algorithm, and text fading is detected. The text fading algorithm compares the color difference between two images, and the mean of the color difference distribution is used as an indicator of the degree of the fading – the fading level is positively correlated with the mean value.



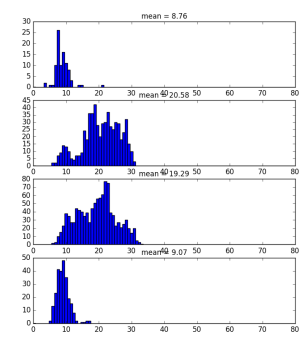
(a) Test page 1



(b) Histogram 1



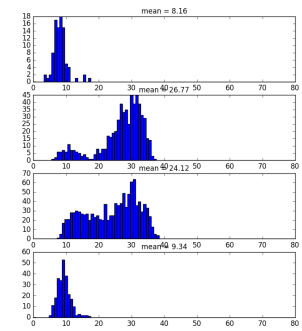
(c) Test page 2



(d) Histogram 2



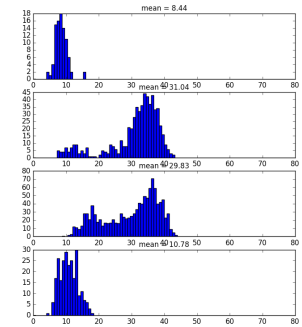
(e) Test page 3



(f) Histogram 3



(g) Test page 4



(h) Histogram 4

Figure 11: Test samples with local analysis.

References

- [1] X. Jing, S. Astling, R. Jessome, E. Maggard, T. Nelson, M. Q. Shaw, and J. P. Allebach, "A General Approach for Assessment of Print Quality," *Image Quality and System Performance X*, SPIE Vol. 8653, P. D. Burns and S. Triantaphillidou, Eds. San Francisco, CA, 3-7 February 2013.
- [2] X. Liu, G. Overall, T. Riggs, R. Silveston-Keith, J. Whitney, G. T. C. Chiu, and J. P. Allebach, "Wavelet-Based Figure of Merit for Macrouniformity," *Image Quality and System Performance X*, SPIE Vol. 8653, P. D. Burns and S. Triantaphillidou, Eds. San Francisco, CA, 3-7 February 2013.
- [3] W. Wang, G. Overall, T. Riggs, R. Silveston-Keith, J. Whitney, G. T. C. Chiu, and J. P. Allebach, "Figure of Merit for Macrouniformity Based on Image Quality Ruler Evaluation and Machine Learning Framework," *Image Quality and System Performance X*, SPIE Vol. 8653, P. D. Burns and S. Triantaphillidou, Eds. San Francisco, CA, 3-7 February 2013.
- [4] M. Q. Nguyen, S. Astling, R. Jessome, E. Maggard, T. Nelson, M. Q. Shaw, and J. P. Allebach, "Perceptual Metrics and Visualization Tools for Evaluation of Page Uniformity," *Image Quality and System Performance XI*, SPIE Vol. 9016, S. Triantaphillidou and M.-C. Larabi, Eds. San Francisco, CA, 3-5 February 2014.
- [5] M. Q. Nguyen and J. P. Allebach, "Controlling Misses and False Alarms in a Machine Learning Framework," *Image Quality and System Performance XII*, SPIE Vol. 9396, M.-C. Larabi and S. Triantaphillidou, Eds. San Francisco, CA, 8-12 February 2015.
- [6] Weibao Wang, Y. Guo, and J. P. Allebach, "Image Quality Evaluation Using Image Quality Ruler and Graphical Model," *Proceedings of ICIP-2015 IEEE International Conference on Image Processing*, Quebec City, Canada, 27-30 September 2015
- [7] S. Hu, H. Nachlieli, D. Shaked, S. Shiffman, and J. P. Allebach, "Color- Dependent Banding Characterization and Simulation on Natural Document Images," *Color Imaging XVII: Displaying, Processing, Hardcopy, and Applications*, SPIE Vol. 8292, R. Eschbach, G. Marcu, and A. Rizzi, Eds., San Francisco, CA, 23-26 January 2012.
- [8] X. Jing, H. Nachlieli, D. Shaked, S. Shiffman, and J. P. Allebach, "Masking Mediated Print Defect Visibility Predictor," *Image Quality and System Performance IX*, SPIE Vol. 8293, F. Gaykema and P. D. Burns, Eds, San Francisco, CA, 23-26 January 2012.
- [9] J. Zhang, H. Nachlieli, D. Shaked, S. Shiffman, and J. P. Allebach, "Psychophysical Evaluation of Banding Visibility in the Presence of Print Content," *Image Quality and System Performance IX*, SPIE Vol. 8293, F. Gaykema and P. D. Burns, Eds, San Francisco, CA, 23-26 January 2012.
- [10] J. Zhang, S. Astling, R. Jessome, E. Maggard, T. Nelson, M. Q. Shaw, and J. P. Allebach, "Assessment of Presence of Isolated Periodic and Aperiodic Bands in Laser Electrophotographic Printer Output," *Image Quality and System Performance X*, SPIE Vol. 8653, P. D. Burns and S. Triantaphillidou, Eds. San Francisco, CA, 3-7 February 2013.
- [11] J. Zhang and J. P. Allebach, "Estimation of Repetitive Interval of Periodic Bands in Laser Electrophotographic Printer Output," *Image Quality and System Performance XII*, SPIE Vol. 9396, M.-C. Larabi and S. Triantaphillidou, Eds. San Francisco, CA, 8-12 February 2015.
- [12] X. Jing, S. Astling, R. Jessome, E. Maggard, T. Nelson, M. Shaw, and J. P. Allebach, "Electrophotographic Ghosting Detection and Evaluation," *Proceedings of NIP-31 IS&T 2015 Conference on Digital Fabrication and Digital Printing*, Portland, OR, 27 September – 1 October 2015.
- [13] J. Wang, T. Nelson, R. Jessome, S. Astling, E. Maggard, M. Shaw, and J. Allebach, "Local Defect Detection and Print Quality Assessment," *International Congress of Imaging Science (ICIS)*, Tel Aviv, Israel, 12-14 May 2014.
- [14] J. Wang, T. Nelson, R. Jessome, S. Astling, E. Maggard, M. Q. Shaw, and J. P. Allebach, "Local Defect Detection and Print Quality Assessment," *Image Quality and System Performance XIII (Part of IS&T Electronic Imaging 2016)*, R. Jenkin and M.-C. Larabi, Eds. San Francisco, CA, 14-18 February 2016.
- [15] N. Yan, E. Maggard, R. Fothergill, R. J. Jessome, and J. P. Allebach, "Autonomous Detection of ISO Fade Point with Color Laser Printers," *Image Quality and System Performance XII*, SPIE Vol. 9396, M.-C. Larabi and S. Triantaphillidou, Eds. San Francisco, CA, 8-12 February 2015.
- [16] Y. Ju, E. Maggard, R. J. Jessome, and J. P. Allebach, "Autonomous Detection of Text Fade Point with Color Laser Printers," *Image Quality and System Performance XII*, SPIE Vol. 9396, M.-C. Larabi and S. Triantaphillidou, Eds. San Francisco, CA, 8-12 February 2015.
- [17] W. Wang, P. Bauer, J. K. Wagner, and J. P. Allebach, "MFP Scanner Diagnostics Using Self-Printed Target to Measure the Modulation Transfer Function," *Image Quality and System Performance XI*, SPIE Vol. 9016, S. Triantaphillidou and M.-C. Larabi, Eds. San Francisco, CA, 3-5 February 2014.
- [18] M. Kim, J. P. Allebach, P. Bauer, and J. K. Wagner, "MFP Scanner Motion Characterization Using Self-Printed Target," *Image Quality and System Performance XII*, SPIE Vol. 9396, M.-C. Larabi and S. Triantaphillidou, Eds. San Francisco, CA, 8-12 February 2015.
- [19] S. B. Reddy and B. N. Chatterji, "An FFT-based Technique for Translation, Rotation and Scale-invariant Image Registration," *IEEE Transactions on Image Processing*, vol. 5, no. 8, August 1996.
- [20] G. Wohlberg and S. Zokai, "Robust Image Registration Using Log-polar Transform," *Image Processing, 2000. Proceedings. 2000 International Conference on*, Vancouver, BC, Canada, September 2000, pp. 493-496(1).
- [21] A. Ardeshir Goshtasby, "2-D and 3-D Image Registration for Medical, Remote Sensing, and Industrial Applications," Wiley Press, 2005
- [22] C. Harris and M. Stephens, "A Combined Corner and Edge Detector," in *Proceedings of the 4th Alvey Vision Conference*, September 1988.
- [23] Y. Lv, Q. Feng, L. Qi and Q. Chen, "Sub-pixel Surface Fitting Algorithm in Digital Speckle Correlation Method," in *The Ninth International Conference on Electronic Measurement & Instruments*, August 2009.
- [24] J. Li and N. M. Allinson, "A Comprehensive Review of Current Local Features for Computer Vision," *Journal of Neurocomputing*, vol. 71, no. 10-12, June 2008.
- [25] R. Hartley and A. Zisserman, "Chapter 4. Estimation – 2D Projective Transformations," in *Multiple View Geometry in*

Computer Vision, 2nd Edition ed., Cambridge University Press, 2004, pp. 87-131.

- [26] Martin A. Fischler and Robert C. Bolles, "Random Sample Consensus: A Paradigm for Model Fitting with Applications to Image Analysis and Automated Cartography," *Communications of the ACM*, vol. 24, no. 6, June 1981.
- [27] P. Torr and A. Zisserman, "MLESAC: A New Robust Estimator with Application to Estimating Image Geometry," *Journal of Computer Vision and Image Understanding*, vol. 78, no. 1, April 2000.